Journal of Alloys and Compounds 587 (2014) 10–13

Contents lists available at ScienceDirect

Journal of Alloys and Compounds

journal homepage: www.elsevier.com/locate/jalcom

Low-temperature large magnetocaloric effect in the antiferromagnetic CeSi compound

L.C. Wang [a], Q.Y. Dong [b], J. Lu [a], X.P. Shao [a], Z.J. Mo [c], Z.Y. Xu [a], J.R. Sun [a], F.X. Hu [a], B.G. Shen [a,*]

[a] State Key Laboratory for Magnetism, Institute of Physics, Chinese Academy of Sciences, Beijing 100190, China
[b] Department of Physics, Capital Normal University, Beijing 100048, China
[c] School of Material Science and Engineering, Hebei University of Technology, Tianjin 300401, China

ARTICLE INFO

Article history:
Received 26 August 2013
Received in revised form 22 October 2013
Accepted 23 October 2013
Available online 31 October 2013

Keywords:
CeSi
Antiferromagnetic
Metamagnetic transition
Magnetocaloric effect
Quartet ground state

ABSTRACT

Magnetic properties and magnetocaloric effect (MCE) of the CeSi compound are investigated. The compound is determined to be antiferromagnet with the Néel temperature $T_N = 6.1$ K. A metamagnetic transition from antiferromagnetic (AFM) to ferromagnetic (FM) state occurs at 2 K under an applied magnetic field of 4 kOe. Field variation generates a large MCE and no magnetic hysteresis loss is observed. The maximum values of magnetic entropy change (ΔS) are found to be −7.2 J/kg K and −13.7 J/kg K for the field changes of 0–20 kOe and 0–50 kOe, respectively. The large ΔS with no hysteresis loss as well as low price of crude materials make CeSi a competitive candidate for low temperature magnetic refrigerant. In addition, the unusual magnetism in CeSi can be attributed to the appearance of a quartet ground state.

1. Introduction

Nowadays, magnetocaloric effect (MCE) technology plays an important role in the refrigeration area for its high energy-efficiency and eco-friendly characteristics, especially compared with the traditional common gas-compression refrigeration [1–4]. After the discovery of $Gd_5Si_2Ge_2$ [5], many researchers devoted their energy to seek for materials with excellent performance and $La(Fe,Si)_{13}$ [6], $MnAs_{1-x}Sb_x$ [7], $MnFeP_{1-x}As_x$ [8] and NiMn based heusler alloys [9] have been reported one after the other. The MCE materials working at room temperature can prevent the emission of green house gases. On the other hand, the materials working at low temperature regime is suitable for the gas liquidation and can help the facility to reach millikelvin [10]. Until now, only the paramagnetic salts as $Gd_3Gd_5O_{12}$, $GdLiF_4$ or GdF_3 have been commercially used [11]. Different with the paramagnetic salts that with small MCE, rare earth-transition metal intermetallic compounds with ferromagnetic (FM) to paramagnetic (PM) transition or antiferromagnetic (AFM) to FM metamagnetic transition are thought to possess large MCE, and series of materials have been reported [12,13]. Generally speaking, the magnitude of MCE is charactered by the isothermal magnetic entropy change or the adiabatic temperature change under the variation of the magnetic field [1–9]. In this paper, we pick up CeSi with AFM order to investigate its magnetic and MCE properties, and a large ΔS without hysteresis loss in terms of low transition temperature (6.1 K) make this material a potential refrigerant in low temperature.

* Corresponding author. Tel.: +86 010 82648082.
E-mail address: shenbg@aphy.iphy.ac.cn (B.G. Shen).

0925-8388/$ - see front matter © 2013 Elsevier B.V. All rights reserved.
http://dx.doi.org/10.1016/j.jallcom.2013.10.183

2. Material and methods

The CeSi ingot was prepared by arc melting method with the stoichiometric starting materials (Ce and Si) on a water-cooled copper crucible under the protection of high-purity argon atmosphere. The purity of all the constituent metals are better than 99.9 wt.%. 2 wt.% excessive Ce was added for the purpose to make up the weight loss during the arc melting. The sample was turned over and remelted for several times to ensure homogeneity. The as-cast ingot was sealed in a quartz tube fulfilled with high-purity argon atmosphere and then annealed at 1223 K for 7 weeks. D2 powder X-ray diffractometer from Bruker Inc. by using Cu Kα radiation was employed to determine the lattice parameter and phase composition. The DC magnetization as a function of temperature and magnetic field were performed on a small piece of the sample by using a commercial superconducting quantum interference device magnetometer (SQUID, Quantum Design).

3. Results and discussion

Fig. 1 shows the standard θ–2θ powder X-ray diffraction patterns for CeSi sample collected at room temperature. The black pattern is the data collected using the Bruker D2 diffractometer and the red line is the standard patterns of CeSi in the PDF data base (PDF#65-1004). It reveals that all the peaks can be indexed and the sample crystallized in a clean phase orthorhombic FeB-type structure (space group: *pnma*; NO. 62) as reported before

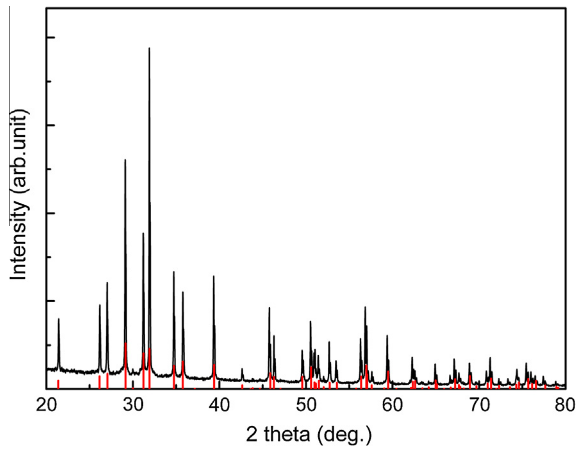

Fig. 1. XRD spectrum for the CeSi alloy.

[14,15]. Within the experimental error, the lattice parameters *a*, *b* and *c* are determined to be 8.305, 3.966 and 5.963 Å, respectively, consistent well with the results in Refs. [14,15].

Fig. 2 displays the temperature dependence of magnetization (*M*–*T*) both under zero-field cooling (ZFC) and field-cooling (FC) modes with a magnetic field of 0.1 kOe, for the purpose to determine the transition temperature and the ground state of the sample. It can be found that each of the ZFC and FC curve exhibits a peak around 6.1 K, which is generally thought to be a striking feature of magnetic transition from AFM to PM state. The AFM nature is in accordance with the earlier reports and the Néel temperature T_N agrees excellently with the results in other published papers [16–19]. This ascertains the sample purity in our experiment indirectly. The reciprocal of susceptibility ($1/\chi$) under ZFC mode as a function of temperature obtained at 0.1 kOe is plotted in the inset of Fig. 2. For obtaining the accurate value of θ_p, the data were collected up to 150 K, while the data for *M*–*T* curves in Fig. 2 were just shown up to 50 K for a clearly visible of the transition temperature. It can be seen that the $1/\chi$ obeys the Curie–Weiss law in the PM region with an effective magnetic moments $\mu_{\rm eff} = 2.53\ \mu_B$, which is close to the free ion value of Ce^{3+} (2.54 μ_B). On the other hand, the paramagnetic Curie temperature (θ_p) derived from the Curie–Weiss fit in the paramagnetic span is equal to 12 K. Generally speaking, negative values of θ_p are always found in samples with anti-ferromagnetic ordering. The unusual positive value of θ_p comes from the appearance of a quartet ground state in spite of a non-cubic crystal symmetry of this compound [19].

Fig. 3(a) and (b) exhibit the magnetic hysteresis loop at 2 K and initial magnetization curves in a temperature range of 2–7 K, for magnetic fields up to 50 kOe respectively. The magnetic hysteresis loop at 2 K shows a negligible hysteresis effect, which is very favorable for the actual application of magnetic refrigerant. The inset of Fig. 3(a) shows the magnified part of the hysteresis loop under magnetic field up to 15 kOe and a clear change in the slope of the curve can be observed under a field of 4 kOe as the earlier report, [17] which indicates a possible metamagnetic transition from AFM to FM state under this magnetic field. On the other hand, the magnetization shows a trend towards saturation between 12 kOe to 50 kOe. The saturation magnetic moment derived from the law of approach to saturation (LATS) is 1.46 μ_B, which is closer to 1.56 μ_B for a Γ_8 quartet rather than a value of 0.71 μ_B for a Γ_7 doublet that has been reported in Ref. [19]. Fig. 3(b) exhibits the field dependence of magnetization in a temperature range from 2 to 7 K with an increment of 1 K, in magnetic fields ranging from 0 to 50 kOe. It can be seen from Fig. 3(b) that there exist crossover among the curves after a careful examination, which ensures the existence of AFM ordering in this compound below T_N [20]. For a general acquaintance of the magnetism of CeSi, a phase diagram is proposed and shown in Fig. 4. It can be seen that the transition field (H_{trs}) for metamagnetic transition decreases with the increasing temperature. The SPM in Fig. 4 indicates a micromagnetic state

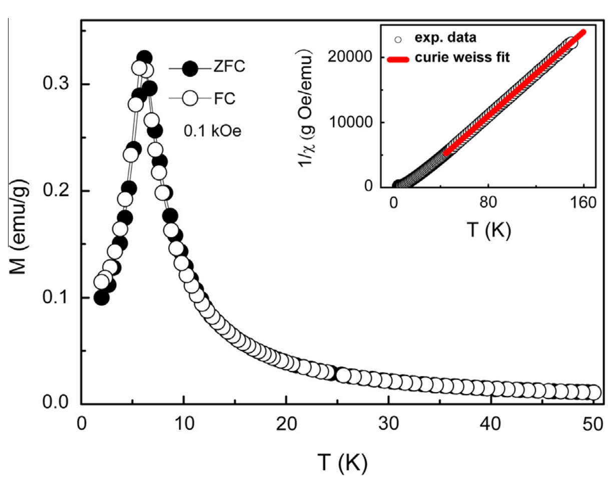

Fig. 2. Temperature dependences of magnetization measured in ZFC and FC modes for CeSi compound. The inset displays the temperature variation of the inverse susceptibility fitted to the Curie–Weiss law.

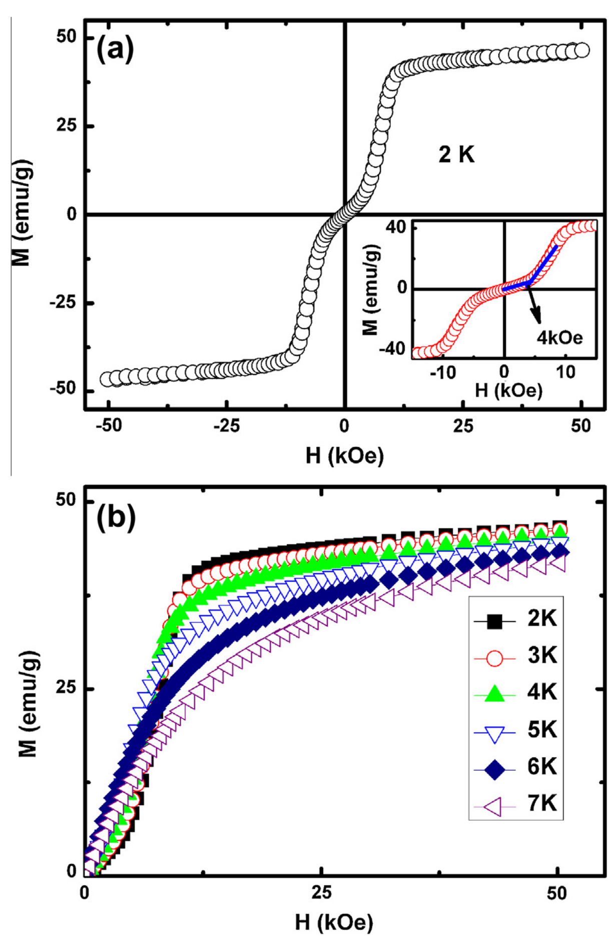

Fig. 3. Magnetic hysteresis loop at 2 K up to 50 kOe, with the inset showing the enlarged part of magnetic hysteresis loop (a) and initial isothermal magnetization curve at typical temperatures (b).

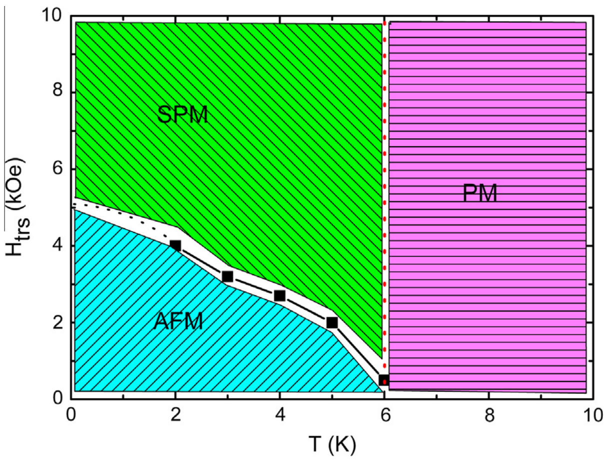

Fig. 4. Proposed magnetic phase diagram of CeSi.

or the intermediate state between the transition from the AFM state to FM state.

The isothermal magnetization curves (*M*–*H*) measured around T_N are shown in Fig. 5(a). The *M*–*H* curves were measured in a heating mode under applied fields up to 50 kOe. Fig. 5(b) presents Arrott-plots (M^2 VS H/M) for CeSi compound measured at typical temperatures. The negative slope of the Arrott plot below T_N, which is presented in Fig. 5(b) and its inset, further confirm the occurrence of a first order AFM-to-FM phase transition according to the Banerjee criterion [21].

The isothermal magnetic entropy changes have been calculated from the isothermal magnetization data by employing Maxwell's relationship $\Delta S = \int_0^H (\partial M/\partial T)_H dH$. The ΔS for different magnetic field changes as a function of temperature (ΔS–T) is shown in Fig. 6. Fig. 6(a) shows the ΔS–T graph under magnetic field changes ranging from 0 to 10 kOe with an increment of 2 kOe. Corresponding to that, Fig. 6(b) shows the ΔS–T graph under magnetic field changes ranging from 10 to 50 kOe with an increment of 10 kOe. One can clearly see that positive values of ΔS are obtained for CeSi in low temperature range as shown in Fig. 6(a), coordinating with the AFM nature of this sample. It can be seen from Fig. 6(b) that the ΔS of CeSi show peaks around T_N and the maximum values of ΔS are found to be −7.2 J/kg K and −13.7 J/kg K for the field changes of 0–20 kOe and 0–50 kOe, respectively. What catches our attentions is that the peak values of ΔS for CeSi can compete with the other popularly researched magnetic refrigerant materials DyCoAl (−16.3 J/kg K), $GdPd_2Si$ (−8.6 J/kg K), RNi_5 (~8 J/kg K) and $ErRu_2Si_2$ (17.6 J/kg K) in low temperature regime under the same field changes [22–25]. Even though the performance of this material is not as good as $ErCo_2$ [26], taking into account of the T_N as low as 6.1 K, the ΔS together with no hysteresis loss, make CeSi an potential candidate for low temperature magnetic refrigerant. There is one point that we should pay extraordinary attention is the indeed low price of Ce and Si compared with the other materials containing Co and heavy rear-earth elements. This is good for the

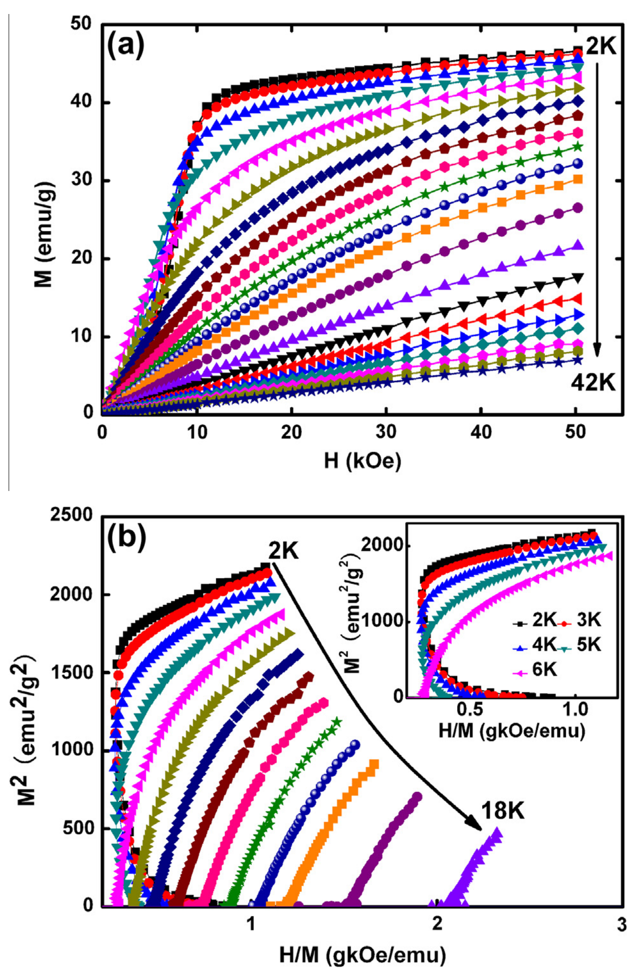

Fig. 5. Magnetic isothermals (a) and Arrott-plots (b) of CeSi measured during field increasing. The inset displays the Arrott plots at temperatures from 2 K to 6 K.

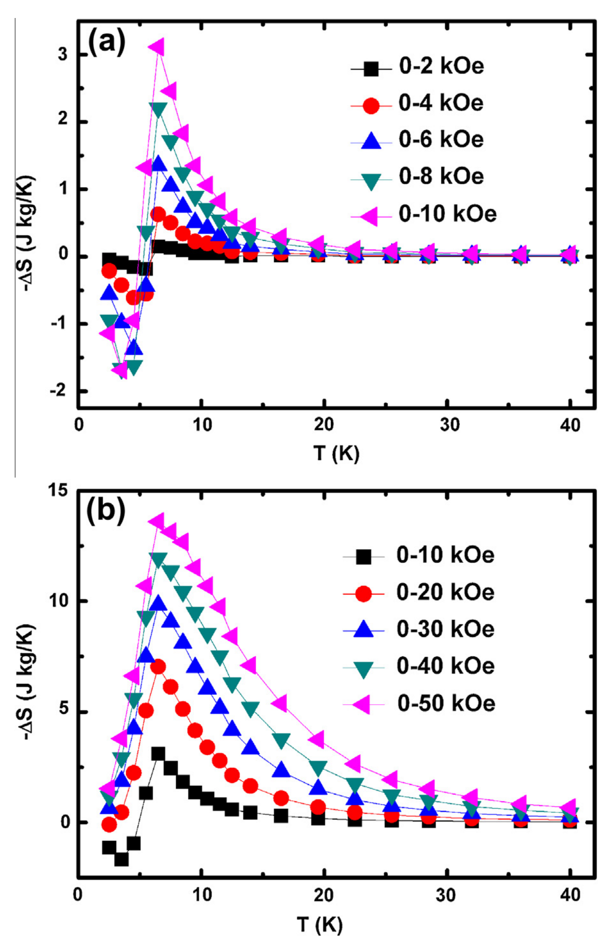

Fig. 6. Magnetic entropy changes as a function of temperature for CeSi compound under various magnetic field changes up to 10 kOe (a) up to 50 kOe (b).

commercial mass production in the future. In addition, the value of ΔS as -13.7 J/kg K, which is very close to Rln4 (-11.6 J/kg K) that corresponds to a quartet ground state. Taking into account the positive value of θ_p and saturation magnetic moment as 1.46 μ_B, the Kondo effect can be excluded and the ground state of CeSi can be attributed to the Γ_8 quartet excited state [17,19].

4. Conclusions

In summary, the magnetic and MCE properties of CeSi with high purity were investigated. The sample crystallized in an orthorhombic FeB-type structure with AFM ordering below T_N = 6.1 K. A metamagnetic transition from AFM-to-FM phase below T_N occurs at 2 K under an applied magnetic field of 4 kOe. The unique magnetism in CeSi that differs greatly from the other Ce compounds can be attributed to the appearance of a quartet ground state. The field-induced metamagnetic transition lead to a large MCE and no magnetic hysteresis loss is observed. The maximum values of magnetic entropy change (ΔS) are found to be -7.2 J/kg K and -13.7 J/kg K for the field changes of 0–20 kOe and 0–50 kOe, respectively. On the other hand, the prices of the crude materials of Ce and Si are much lower than the other potential materials containing Co and heavy rear-earth elements. All these merits make CeSi a competitive candidate for low temperature (<10 K) magnetic refrigerant.

Acknowledgements

This work was supported by the National Natural Science Foundation of China (11274357, 51021061 and 51271196), the Key Research Program of the Chinese Academy of Sciences, the Hi-Tech Research and Development program of China (2011AA03A404), and the National Basic Research Program of China (2010CB 833102), and is a part of the Beijing Excellent talent training support (Grant No. 2012D005016000002).

References

[1] K.A. Gschneidner Jr., V.K. Pecharsky, A.O. Tsokol, Rep. Prog. Phys. 68 (2005) 1479–1539.
[2] V. Franco, J.S. Blázquez, A. Conde, Appl. Phys. Lett. 89 (2006). 222512-1-3.
[3] B.G. Shen, J.R. Sun, F.X. Hu, H.W. Zhang, Z.H. Cheng, Adv. Mater. 21 (2009) 4545–4564.
[4] B.G. Shen, F.X. Hu, Q.Y. Dong, J. R Sun, Chin. Phys. B 22 (2013). 017502-1-11.
[5] V.K. Pecharsky, K.A. Gschneidner Jr., Phys. Rev. Lett. 78 (1997) 4494–4497.
[6] F.X. Hu, B.G. Shen, J.R. Sun, X.X. Zhang, Chin. Phys. 9 (2000) 550–553.
[7] H. Wada, Y. Tanabe, Appl. Phys. Lett. 79 (2001) 3302–3304.
[8] O. Tegus, E. Bruck, K.H.J. Buschow, F.R. de Boer, Nature (London) 415 (2002) 150–152.
[9] F.X. Hu, B.G. Shen, J.R. Sun, Chin. Phys. B 22 (2013). 037505-1-15.
[10] A.M. Tishin, Y.I. Spichkin, in: J.M.D. Coey, D.R. Tilley, D.R. Vij (Eds.), The Magnetocaloric Effect and its Applications, Institute of Physics Publishing, Bristol, 2003.
[11] J.A. Barclay, W.A. Steyert, Cryogenics 22 (1982) 73–80.
[12] J. Chen, B.G. Shen, Q.Y. Dong, F.X. Hu, J.R. Sun, Appl. Phys. Lett. 96 (2010). 152501-1-3.
[13] D.X. Li, T. Yamamura, S. Nimori, Y. Homma, F. Honda, D. Aoki, Appl. Phys. Lett. 102 (2013). 152409-1-4.
[14] Edgar. Cordruwisch, Dariusz. Kaczorowski, Peter. Rogl, Adriana. Saccone, Riccardo. Ferro, J. Alloys Comp. 320 (2001) 308–319.
[15] M.V. Bulanova, P.N. Zheltov, K.A. Meleshevich, P.A. Saltykov, G. Effenberg, J. Alloys Comp. 345 (2002) 110–115.
[16] X. Xu, S.A. Shaheen, Peggy Hill, Naushad Ali, J. Alloys Comp. 181 (1992) 305–309.
[17] S.A. Shaheen, J. Appl. Phys. 63 (1988) 3411–3413.
[18] S.A. Shaheen, J.S. Schilling, Phys. Rev. B: Condens. Matter 35 (1987) 6880–6887.
[19] S.A. Shaheen, Phys. Rev. B: Condens. Matter 36 (1987) 5472–5475.
[20] Niraj.K. Singh, K.G. Suresh, R. Nirmala, A.K. Nigam, S.K. Malik, J. Magn. Magn. Mater. 302 (2006) 302–305.
[21] S.K. Banerjee, Phys. Lett. 12 (1964) 16–17.
[22] R. Rawat, I. Das, J. Phys.: Condens. Matter 13 (2001) L57–L63.
[23] X.X. Zhang, F.W. Wang, G.H. Wen, J. Phys.: Condens. Matter 13 (2001) L747–L752.
[24] P.J. von Ranke, M.A. Mota, D.F. Grangeia, A. Magnus, G. Carvalho, F.C.G. Gandra, A.A. Coelho, A. Caldas, N.A. de Oliveira, S. Gama, Phys. Rev. B 70 (2004). 134428-1-6.
[25] T. Samanta, I. Das, S. Banerjee, Appl. Phys. Lett. 91 (2007). 152506-1-3.
[26] H. Wada, Y. Tanabe, M. Shiga, H. Sugawara, H. Sato, J. Alloys Comp. 316 (2001) 245–249.